Theoretical Study of the Nature of the Bonding in $[Cp_2M(\mu\text{-}X)]_2$, Where M = Zr (X = I, PH_2, and NH) and M = Ti (X = Cl)

Roger L. DeKock,*,† Michael A. Peterson,† Lewis E. L. Reynolds,† Li-Heng Chen,†,‡ Evert Jan Baerends,§ and Pieter Vernooijs§

Departments of Chemistry, Calvin College, Grand Rapids, Michigan 49546, and Free University, De Boelelaan 1083, 1081HV Amsterdam, The Netherlands

Received June 2, 1992

We have completed Hartree–Fock–Slater quantum chemical studies on the title molecules in order to examine the nature of the metal–metal and metal–ligand bonding in these complexes. Our results indicate that the highest occupied molecular orbital produces a Zr(III)–Zr(III) bond for X = I, PH_2. This contradicts the interpretation of the X-ray structure: namely, that there is no Zr–Zr bond since the intermetallic distance of ~3.65 Å is 0.4–0.5 Å longer than for "typical" Zr–Zr single bonds. But for a number of reasons we are loathe to give this bond the status of a "single" bond and instead assign it a bond order of about 0.5. The Zr–Zr distance for the imido complex is ~3.20 Å, even though it is formally Zr(IV) and there can be no formal Zr–Zr bond. Our results indicate that the Zr–Zr distance results from the interplay between the Zr–X bridge bonds, the metal–metal bond, and the steric interaction between the four Cp rings. The last point is corroborated by selected molecular mechanics calculations on various configurations of the four Cp ligands. Studies on model dication and dianion systems illustrate how the Cp rings function as electron "buffers" by keeping the effective electronic charge in the M_2X_2 portion of the molecule roughly constant. The magnetic properties and the absence of a Ti(III)–Ti(III) bond for the Ti compound are briefly discussed.

Introduction

We have used Hartree–Fock–Slater, molecular mechanics, and Fenske–Hall theoretical methods in order to better understand the electronic and steric factors that determine the geometrical structures and magnetic properties of the title molecules. The initial impetus for this work was provided by the anomalously long Zr–Zr distances of these dinuclear systems involving bridging main-group atoms. But from that initial work, we extended it to an examination of the steric effects of the Cp ligands, the effect that the size of the bridging ligands has upon the Zr–Zr distance, and the effect of Zr(III) vs Zr(IV). In addition, we studied dications and dianions of selected dinuclear Zr systems in order to provide more insight into the nature of the HOMO and LUMO for these complexes. Finally, we examined the electronic structure of the title Ti complex, in order to provide a comparison between a first-row and second-row dinuclear transition-metal complex.

Chiang, Gambarotta, and van Bolhuis[1] reported the synthesis and X-ray structure of $\{Cp_2Zr[\mu\text{-}P(CH_3)_2]\}_2$ (1), in which they interpreted the long Zr–Zr distance (3.653 Å) as indicating the absence of a metal–metal bond. For such a Zr(III) species the d^1 electron count is sufficient to provide for a metal–metal bond and at the same time achieve an 18-electron count for each Zr. Long Zr–Zr distances were found also for a similar complex with one bridging Cl and one bridging $P(CH_3)_2$ ligand,[1] for $\{Cp_2Zr(\mu\text{-}I)\}_2$[2] (2), and for $[(C_5H_4Me)_2Zr(\mu\text{-}I)]_2$.[3] Magnetic susceptibility and NMR measurements, where available, indicate diamagnetic complexes and therefore spin pairing of the electrons in these complexes.

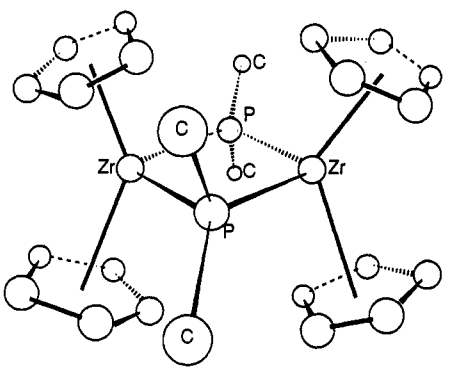

1

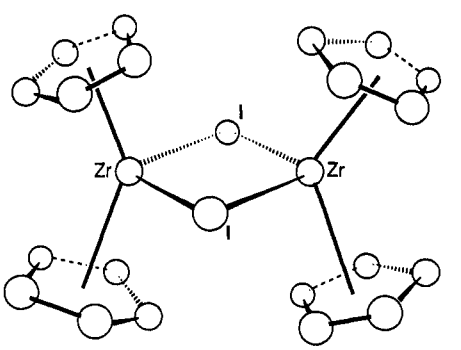

2

† Calvin College.
‡ Permanent address: Aquinas College, Grand Rapids, MI 49506.
§ Free University.

(1) Chiang, M. Y.; Gambarotta, S.; van Bolhuis, F. *Organometallics* **1988**, *7*, 1864.
(2) Wielstra, Y.; Gambarotta, S.; Meetsma, A.; de Boer, J. L. *Organometallics* **1989**, *8*, 250.
(3) Wielstra, Y.; Gambarotta, S.; Meetsma, A.; Spek, A. L. *Organometallics* **1989**, *8*, 2948.

0276-7333/93/2312-2794$04.00/0

Other Zr(III) compounds have two of the "Cp" rings fused into the fulvalene ligand. One such compound[4] with bridging Cl ligands has a much shorter Zr–Zr distance of 3.233 Å; another[3] with (X = μ-I) has a Zr–Zr distance of 3.472 Å and a third[5] (X = μ-SPh) exhibits a Zr–Zr distance of 3.420 Å. The first was stated to have a Zr–Zr bond whereas the latter two were stated to have no Zr–Zr bond.

There are many experimental indicators of "typical" Zr–Zr distances and these usually are in the range 3.1–3.2 Å.[4,6] For example, a complex of the edge-sharing bioctahedron type without bulky ligands, $[Cl_2(PMe_2Ph)_2Zr(\mu\text{-}Cl)]_2$, has a Zr(III)–Zr(III) distance of 3.127 Å.[6a] The distances in the shared octahedra of $ZrCl_3$ and $ZrBr_3$ are 3.069 and 3.152 Å, respectively.[7] The structure of ZrI_3 recently has been revised to show that it consists of confacial ZrI_6 octahedra with alternating long and short Zr–Zr distances of 3.172 and 3.507 Å, respectively.[7] The former distance is interpreted as indicating metal dimers, and the latter, as a nonbonding distance. In 1990 two Hf(III)–Hf(III) distances were found by X-ray to be near 3.10 Å, again in the absence of bulky ligands.[8] Since Hf and Zr have roughly the same radii, this is to be expected.

Of course, all of this attention to the Zr–Zr distance alone does not take into consideration the oxidation state of the Zr or the size of the bridging ligands or the Cp ligands, and these are factors that we now address.

Erker et al.[9] have studied a pair of Zr(III) dimers which show that the size of the bridging ligand is extremely important in determining the distance between the metal atoms. The two complexes are $[(Me_3CCp)_2Zr(\mu\text{-}Te)]_2$ where the Zr–Zr distance is 4.067 Å and $[(Me_3CCp)_2Zr]_2(\mu\text{-}Te)(\mu\text{-}O)$ where the Zr–Zr distance is 3.390 Å. Another pair of complexes that show the importance of the size of the bridging ligand is provided by the edge-sharing bioctahedron complexes $[X_2(PMe_2Ph)_2Zr(\mu\text{-}X)]_2$, which have a Zr(III)–Zr(III) distance of 3.439 Å[6b] for X = I; this shortens to 3.127 Å for X = Cl.[6a] An interesting structural comparison also is provided by Zr(IV) dimers. Bottomley[10] and co-workers have determined the X-ray structure of $[Cp_2Zr(\mu\text{-}S)]_2$ (**3**), and found the Zr–Zr distance to be 3.530

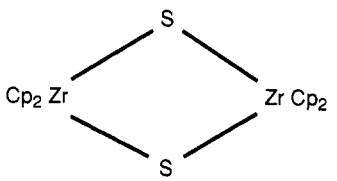

3

Å. By comparing **1** and **3** we see that going from Zr(III) with a bridging phosphido ligand to Zr(IV) with bridging sulfido shortens the Zr–Zr distance by about 0.1 Å.

Another Zr(IV) dimer (**4**), but with a bridging first-row

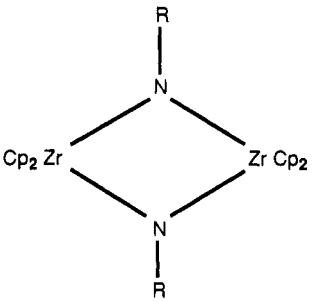

4

imido ligand, exhibits a Zr–Zr distance near 3.2 Å.[11] Comparing **1** and **4**, we see that a formal Zr–Zr single bond can be ~0.5 Å *longer* than the distance found in a complex without a formal Zr–Zr bond. Another important aspect is that the "bite" angle of the bridging ligand must be flexible, as it is for μ-PR_2.[12]

We turn next to the steric effect of the Cp ligand and its derivatives. We quote from du Plooy et al.[13] "The η^5-bonded cyclopentadienyl ring occupies three coordination sites when bonded to transition metals and relative to three monosubstituted ligands is regarded as a small ligand. Consequently, in most discussions involving the cyclopentadienyl ligand emphasis has been placed on the electronic rather than the steric effects of the ligand." There are three structural parameters that are of importance for the Cp ligand, as shown in **5**. These are the metal to Cp centroid (CNT) distance R, the CNT–M–CNT angle θ, and the Cp "tilt" angle τ.

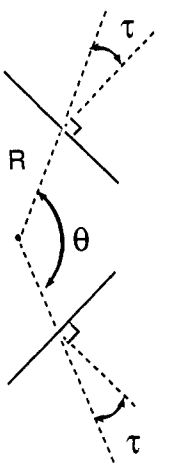

5

In compounds involving the Cp_2Zr fragment, the Cp rings are sometimes found to be eclipsed and other times staggered.[14] There is no evident correlation between these conformations and other geometric features. Ring conformations may be controlled mainly by crystal packing

(4) Gambarotta, S.; Chiang, M. Y. *Organometallics* **1987**, *6*, 897.
(5) Wielstra, Y.; Gambarotta, S.; Spek, A. L.; Smeets, W. J. J. *Organometallics* **1990**, *9*, 2142.
(6) (a) Cotton, F. A.; Diebold, M. P.; Kibala, P. A. *Inorg. Chem.* **1988**, *27*, 799. The quoted bond distance is an average of two independent molecules in the unit cell. (b) Cotton, F. A.; Shang, M.; Wotczak, W. A. *Inorg. Chem.* **1991**, *30*, 3670.
(7) Lachgar, A.; Dudis, D. S.; Corbett, J. D. *Inorg. Chem.* **1990**, *29*, 2242.
(8) Morse, P. M.; Wilson, S. R.; Girolami, G. S. *Inorg. Chem.* **1990**, *29*, 3200. Cotton, F. A.; Kibala, P. A.; Wotczak, W. A. *Inorg. Chim. Acta* **1990**, *177*, 1.
(9) Erker, G.; Nolte, R.; Tainturier, G.; Rheingold, A. *Organometallics* **1989**, *8*, 454.
(10) Bottomley, F.; Drummond, D. F.; Egharevba, G. O.; White, P. S. *Organometallics* **1986**, *5*, 1620.
(11) Walsh, P. J.; Hollander, F. J.; Bergman, R. G. *J. Am. Chem. Soc.* **1988**, *110*, 8729.
(12) Vahrenkamp, H. *Chem. Ber.* **1978**, *111*, 3472. Vahrenkamp, H. *Angew. Chem., Int. Ed. Engl.* **1978**, *17*, 379. Shaik, S.; Hoffmann, R.; Fisel, C. R.; Summerville, R. H. *J. Am. Chem. Soc.* **1980**, *102*, 4555.
(13) du Plooy, K. E.; Marais, C. F.; Carlton, L.; Hunter, R.; Boeyens, J. C. A.; Coville, N. J. *Inorg. Chem.* **1989**, *28*, 3855.
(14) Cardin, D. J.; Lappert, M. F.; Raston, C. L. *Chemistry of Organozirconium and-hafnium Compounds*; Ellis Horwood: Chichester, England, 1986.

Table I. Pertinent Structural Results for Compounds of This Study

compd	M-M (Å)	M-CNT (Å)	CNT-M-CNT (deg)	M-(μ-X) (Å)
1	3.653	2.22[c]	130[d]	2.6845[b]
2	3.649	2.209	130.13	2.9161[b]
4	3.198	2.265[a]	123.95	2.0955
6	3.9555[a]	2.05[d]	131.77[c]	2.5415

[a] Average of two distances. [b] Average of eight distances. [c] Average of four values. [d] Not published in the original work. This value was estimated by us.

effects. Steric effects relating to Cp ligands have been examined in numerous articles.[9,13,15-21]

Some pertinent structural results for the compounds of this study are presented in Table I. These results are typical in that R is generally in the range 2.20–2.25 Å and θ is in the range 125–140°. The larger values of θ are found for the bulkier ligand η^5-C_5Me_5. Note that the angle θ is more acute in the case of 4 where the four Cp rings are pressed closer together. At the same time the centroid distance R increases in 4 compared to 1. All of these features point to steric congestion among the Cp ligands in these molecules. We do not present tilt angles τ. For these three compounds the tilt angles are in the range 1–2°. The lack of significant tilt angles may be interpreted as evidence for steric congestion on both "sides" of the Cp rings.

We turn next to known information on the title Ti complex, 6; X-ray crystallography indicates a structure analogous to 2 with a Ti–Ti distance of 3.956 Å.[22] Magnetic

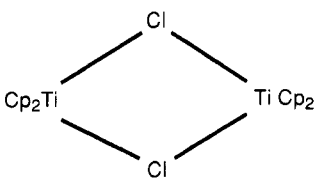

6

susceptibility measurements indicate paramagnetism, specifically antiferromagnetic coupling of the unpaired d^1 electron on each Ti(III).[22] The Ti–Ti distance is longer even than the "long" Zr–Zr distances of 1 and 2. A complex like 6 but with bridging PR_2 groups also is known; it too is paramagnetic and has a Ti–Ti distance of 3.918 Å.[23] There are other reports in the literature wherein dinuclear complexes of Ti(III) are known to be paramagnetic, but those of Zr(III) are diamagnetic.[24] There is one report of a dinuclear Ti(III) complex, $[(OR)_2Ti(\mu\text{-}Cl)]_2$, that has a short Ti–Ti distance of 2.98 Å and is diamagnetic.[25] In comparing 2 and 6, we have one example, of many that are known, where analogous compounds of first- and second-row transition metals exhibit paramagnetism for the first row and diamagnetism for the second row.[26]

It is with this background that we carried out a Hartree–Fock–Slater (HFS) quantum chemical study and some molecular mechanics studies into the nature of the bonding in 1, 2, 4, and 6. The HFS study was done to learn more about the electronic structure of these complexes, and the molecular mechanics study was done to examine more closely the steric effects of the Cp ligands.

While this work was in preparation we were informed of the theoretical studies[27] of M.-M. Rohmer and M. Bénard, who completed extended Hückel work on 2 and ab initio SCF/Cl quantum chemical calculations on 1 and on $[Cl_2(PH_3)_2Zr(\mu\text{-}Cl)]_2$. In brief, our quantum chemical and molecular mechanics work is in agreement with their conclusions that the Zr–Zr distance is controlled by an interplay of metal–metal bonding and steric interactions among the ligands. Our work shows the importance of the metal–bridge interaction, since we examined the electronic structure and bonding in 4, the bridging imido complex, and we examined bond fragmentation energies. We also have examined the bonding from the point of view of several fragments in order to attempt the determination of the strength of the metal–metal interaction. We have performed some studies on dications and dianions of these complexes in order to gain additional insight into the nature of the HOMO/LUMO and how these complexes might behave upon oxidation or reduction. Finally, we studied 6, the Ti(III) complex, so as to compare first- and second-row transition-metal complexes. Near the completion of our work, we were informed that Rohmer and Bénard also had completed a theoretical study into a comparison of the metal–metal bond in dinuclear Ti(III) complexes compared to Zr(III).[28]

Theoretical Method and Geometrical Details

The foundation of the HFS method has been presented in a number of papers.[29] An attractive aspect of this computational package is the ability to obtain theoretical energy differences between the fragments that make up a molecule;[30] whether these fragments are atoms or larger moieties is immaterial. It has been applied extensively in the area of transition-metal chemistry,[31] including an analysis of the nature of metal–metal bonding in dimetallic complexes.[32]

The basis set consisted of uncontracted Slater-type atomic orbitals. The method utilizes the frozen core approximation. The valence orbitals are orthogonalized

(15) Benn, R.; Grondey, H.; Erker, G.; Aul, R.; Nolte, R. *Organometallics* **1990**, *9*, 2493.
(16) Shaver, A.; McCall, J. M.; Day, V. W.; Vollmer, S. *Can. J. Chem.* **1987**, *65*, 1676.
(17) Howard, C. G.; Girolami, G. S.; Wilkinson, G.; Thornton-Pett, M.; Hursthouse, M. B. *J. Am. Chem. Soc.* **1984**, *106*, 2033.
(18) Bottomley, F.; Keizer, P. N.; White, P. S. *J. Am. Chem. Soc.* **1988**, *110*, 137.
(19) Simões, J. A. M.; Beauchamp, J. L. *Chem. Rev.* **1990**, *90*, 629, particularly see p 634.
(20) Xing-Fu, L.; Fischer, R. D. *J. Less-Common Metals* **1985**, *112*, 303.
(21) Xing-Fu, L.; Ao-Ling, G. *Inorg. Chim. Acta* **1987**, *134*, 143.
(22) Jungst, R.; Sekutowski, D.; Davis, J.; Luly, M.; Stucky, G. *Inorg. Chem.* **1977**, *16*, 1645. The quoted bond distance is an average of two independent molecules in the unit cell.
(23) Payne, R.; Hachgenei, J.; Fritz, G.; Fenske, D. *Z. Naturforsch.* **1986**, *41B*, 1535.
(24) Wade, S. R.; Wallbridge, M. G. H.; Willey, G. R. *J. Chem. Soc. D* **1983**, 2555.
(25) Hill, J. E.; Nash, J. M.; Fanwick, P. E.; Rothwell, I. P. *Polyhedron* **1990**, *9*, 1617.
(26) Cotton, F. A.; Wilkinson, G. *Advanced Inorganic Chemistry*, 5th ed.; Wiley-Interscience: New York, 1988; p 632.
(27) M. Bénard, private communication, April 1990. Rohmer, M.-M.; Bénard, M. *Organometallics* **1991**, *10*, 157.
(28) Bénard, M., private communication, February 1992. Bénard, M.; Rohmer, M.-M. *J. Am. Chem. Soc.* **1992**, *114*, 4785.
(29) Baerends, E. J.; Ellis, D. E.; Ros, P. *Chem. Phys.* **1973**, *2*, 41. Baerends, E. J.; Ros, P. *Chem. Phys.* **1973**, *2*, 52. Baerends, E. J.; Ros, P. *Chem. Phys.* **1975**, *8*, 41.
(30) Ziegler, T.; Rauk, A. *Theor. Chim. Acta* **1977**, *46*, 1. Ziegler, T.; Rauk, A. *Inorg. Chem.* **1979**, *18*, 1558.
(31) Baerends, E. J.; Ros, P. *Int. J. Quantum Chem. Symp.* **1978**, *12*, 169. Baerends, E. J.; Rozendaal, A. In *Quantum Chemistry: The Challenge of Transition Metals and Coordination Chemistry*; Veillard, A., Ed.; D. Reidel: Dordrecht, 1986; pp 159–177. Ziegler, T.; Tschinke, V.; Versluis, L.; Baerends, E. J.; Ravenek, W. *Polyhedron* **1988**, *7*, 1625.

Table II. List of Pertinent Geometrical Information and Relative Energies (HFS and MMX) for Our Model Compounds

compd	symmetry	M–M (Å)	M–CNT (Å)	CNT–M–CNT (deg)	H···H (Å) same metal[a]	H···H (Å) diff metal[a]	rel energy (kcal/mol) HFS	rel energy (kcal/mol) MMX
1	C_{2h}	3.65	2.22	130	2.67 (4)	2.24 (4)	0.0	0.0
1	D_{2h}	3.65	2.22	130	2.09 (4)	2.17 (4)	3.5	1.9
2	C_{2h}	3.65	2.22	130	2.67 (4)	2.24 (4)	0.0	0.0
2	D_{2h}	3.65	2.22	130	2.09 (2)	2.17 (4)	3.4	1.9
4	C_{2h}	3.20	2.26	125	2.52 (4)	2.12 (4)	0.0	0.0
4	D_{2h}	3.20	2.26	125	1.90 (2)	2.00 (4)	5.5	9.7
4	C_{2h}	3.20	2.26	130	2.73 (4)	1.92 (4)	4.3	8.8
4	D_{2h}	3.20	2.26	130	2.16 (2)	1.76 (4)	7.8	15.6

[a] The number in parentheses indicates the number of such contacts in the entire model complex.

onto the core by employing a single ζ exponent in the valence set for each core-type orbital. The following orbitals are kept in the core: C (1s); N (1s); P (1s, 2s, 2p); Zr (1s, 2s, 2p, 3s, 3p, 3d); I (1s, 2s, 2p, 3s, 3p, 3d, 4s, 4p, 4d). Notice that eight electrons more than "necessary" have been kept in the valence shell of Zr. We used a valence basis set which is briefly described as follows: H (double ζ, 1s); C and N (double ζ, 2s; double ζ, 2p); P (double ζ, 3s; double ζ, 3p; single ζ, 3d); Cl (double ζ, 3s; double ζ, 3p); Zr (double ζ, 4s; double ζ, 4p; single ζ, 5s; single ζ, 5p; double ζ, 4d); I (double ζ, 5s; double ζ, 5p).

The metrical parameters for the calculation were idealized from the results of the X-ray structures. We assumed idealized Cp rings with a C–C distance of 1.42 Å and a C–H distance of 1.08 Å. For **1** and **2** we chose the Zr–Cp centroid (CNT) distance as 2.22 Å. This provides a Zr–C distance of 2.527 Å. For **4** the corresponding numbers are 2.26 and 2.563 Å. The Zr–Zr distance was chosen to be 3.65 Å for **1** and **2** and 3.20 Å for **4**. The CNT–Zr–CNT angle was taken as 130° for **1** and **2** and 125° for **4**. These values are in good agreement with the X-ray values for these compounds, as described in the Introduction. (In addition, a CNT–Zr–CNT angle of 130° was used for **4**, which was done in order to examine the effect of this angle on the energy.) We assumed the "tilt" angle to be zero in all cases. The Zr–P distance was 2.68 Å. The Zr–N distance was 2.10 Å, and the Zr–I distance was 2.92 Å. For the Ti complex, **6**, we chose the following metrical parameters: a Ti–Cp centroid distance of 2.05 Å (Ti–C distance of 2.379 Å); a Ti–Cl distance of 2.55 Å; a Ti–Ti distance of 3.95 Å; a CNT–Ti–CNT angle of 130°.

The major difference between the theoretical and experimental structures is that we used H substituents on the P and N bridging atoms of **1** and **4** rather than the moieties found in the experimental structures. The local geometry around the P is as follows: P–H distance of 1.44 Å, H–P–H angle of 93°. This P–H bond distance is near the value found in PH_3.[33] In earlier work we found that replacement of CH_3 by an H atom had little effect upon the theoretical results for $P(CH_3)_3$ as a donor ligand compared to PH_3, as long as the interbond angle in the prototype ligand corresponded with the angle in the actual complex.[34] In the present work this is a moot point since the H–P–H angle in PH_3 and the C–P–C angle in **1** are both near our chosen angle of 93°. (However, this says nothing about the possible steric effects that the methyl groups on the bridging phosphido ligands might exert with the Cp rings. We take up this point in our discussion of the molecular mechanics results.) The N–H distance in **4** was chosen to be 1.0 Å. Our metrical parameters for **2** were not taken from ref 2, but rather from the structure of the methyl-substituted cyclopentadienyl compound[3] which was much better resolved.

We now discuss the orientation of the Cp rings with respect to each other. It is clear from the ORTEP diagrams[1,3] of **1** and **2** that the rings are staggered, both in the case of the rings on the same metal atom and in the case of the rings on different metal atoms, as shown in **7**.

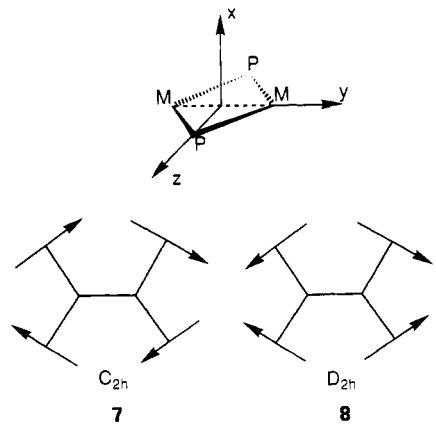

7 **8**

In our idealized structure this molecule has C_{2h} symmetry. We also completed theoretical studies for several of the complexes in which the rings were eclipsed, so that the idealized point group is D_{2h} (**8**). (In these diagrams the arrowhead refers to a CH unit that has a z coordinate of zero, where z is perpendicular to the plane of the paper.) The question of near-neighbor H···H contacts will be important in our discussion, and so we exhibit the values for our model compounds in Table II. It is these structures of Cp rings for which we have undertaken molecular mechanics calculations.[35]

Results and Discussion

Molecular Mechanics, Steric Congestion, and HFS Relative Energies. We first raise the question as to why

(32) Heijser, W.; Baerends, E. J.; Ros, P. *Faraday Symp.* **1980**, *14*, 211. Baerends, E. J.; Post, D. In *Quantum Theory of Chemical Reactions*; Daudel, R.; Pullman, A.; Veillard, A., Eds.; D. Reidel: Dordrecht, 1982; Vol. 3, pp 15–33. Ziegler, T. *J. Am. Chem. Soc.* **1983**, *105*, 7543. Ziegler, T. *J. Am. Chem. Soc.* **1984**, *106*, 5901. Ziegler, T. *J. Am. Chem. Soc.* **1985**, *107*, 4453.

(33) Herzberg, G. *Molecular Spectra and Molecular Structure, III. Electronic Spectra and Electronic Structure of Polyatomic Molecules*; Van Nostrand Rheinhold: New York, 1966.

(34) DeKock, R. L.; Baerends, E. J.; Boerrigter, P. M.; Hengelmolen, R. *J. Am. Chem. Soc.* **1984**, *106*, 3387.

(35) Burkert, U.; Allinger, N. L. *Molecular Mechanics*; American Chemical Society: Washington, DC, 1982. The modeling program that we used was version 3.2 of PCMODEL, available from Serena Software, P.O. Box 3076, Bloomington, IN 47402-3076. The force field is described in a chapter: Gajewski, J. J.; Gilbert, K. E.; McKelvey, J. In *Advances in Molecular Modeling*; Liotta, D., Ed.; Jai Press, Inc.: Greenwich, CT, 1990; Vol. 2, p 65. We are not the first to carry out molecular mechanics calculations on the organic fragments of zirconocene complexes: Stephan, D. W. *Organometallics* **1990**, *9*, 2718. The molecular modeling studies that we completed on the Zr_2X_2 portions of the complexes were done with PCMODEL 4.0.

the Zr–Zr distance in **1** and **2** is near 3.65 Å, whereas a d^0–d^0 (**4**) system can have a length near 3.20 Å? As intimated in the Introduction, we propose that it is the near-neighbor H···H contacts of the H atoms on Cp rings belonging to *different* Zr atoms that cause the long Zr–Zr distance, coupled with the inherently longer Zr–P distance (2.67 Å) and Zr–I distance (2.92 Å) compared to the first-row Zr–N distance (2.10 Å) in the imido complexes. Table II exhibits not only the pertinent H···H contacts but also the relative energies of the various model structures obtained by the HFS method, and the relative energies of the Cp fragments calculated from molecular mechanics. We emphasize that the HFS data in Table II were obtained from quantum chemical studies on the complete complexes as depicted in **1**, **2**, and **4**. However, the data from the molecular mechanics method are only for fixed-geometry Cp rings corresponding to those in **1**, **2**, and **4**. But before we look at near-neighbor H···H contacts from Cp rings on different Zr atoms, we first look at such contacts between Cp rings on the same Zr atom.

Within the Cp_2Zr fragment itself we considered both C_{2v} and C_s symmetries. The former corresponds to an eclipsed and the latter to a staggered arrangement of the two Cp ligands. As expected, the staggered configuration is more stable according to both the HFS calculations and the molecular mechanics model. According to our work, for a fixed CNT–Zr–CNT angle of 130° and a Zr–CNT distance of 2.22 Å, the difference in energy is only about 1 kcal/mol by either method; this indicates that there are no severe H···H repulsions to restrict the rotation. In our fragment the nearest H···H distances are 2.67 Å in C_s and 2.09 Å in C_{2v} symmetry (Table II). The latter distance is in the range of overlapping van der Waals' radii for the H atoms and is no doubt responsible for the small increase in energy.[22,36] Recent NMR work has shown that a substituent larger than the H atom is needed in order to slow down the dynamics of the ring rotation.[9,15]

We now consider the near-neighbor H···H contacts that arise when the two $ZrCp_2$ units are brought together. We can bring the C_s units together in such a way as to make all of the Cp units staggered with respect to each other. This produces a C_{2h} structure, as depicted in **7**. On the other hand, the C_{2v} units can be brought together to produce a structure of D_{2h} symmetry (**8**), in which the Cp units are eclipsed not only on the same Zr but also between different Zr atoms. The geometrical data in Table II show near-neighbor H···H contacts for a number of model complexes with Zr–Zr distances of 3.65 and 3.20 Å, coupled with Zr–CNT distances of 2.22 and 2.26 Å, and CNT–Zr–CNT angles of 125 and 130°. The eclipsed structures (D_{2h}) have nearer contacts across the Zr–Zr framework than do the staggered structures (C_{2h}), as expected. We can immediately see why the CNT–Zr–CNT angle decreases from 130° for Zr–Zr of 3.65 Å to 125° for Zr–Zr of 3.20 Å and why the Zr–CNT distance increases from 2.22 to 2.26 Å for this Zr–Zr shortening. For example, for the C_{2h} structures, the angle change alone has the effect of lengthening the nearest-neighbor contact across the Zr–Zr framework from 1.92 to 2.12 Å. According to our HFS model this lowers the energy by 4.3 kcal/mol, and by 8.8 kcal/mol according to the molecular mechanics model (the latter refers to the Cp rings alone). In general, there is good agreement between the number and distance of near-neighbor contacts and the relative energies of the different model structures shown in Table II. Furthermore, there is good agreement between the HFS relative energies and those obtained by the molecular mechanics work.

Close analysis of these energy differences shows that they are almost exclusively due to the van der Waals' energy component of the "strain energy" that is output from the MMX force field of PCMODEL. We quote here the value of this vdw term for each of the C_{2h} structures in the order they are reported in Table II: −0.5, −0.5, +7.0, and +15.8 kcal/mol. Hence, it is clear that the vdw changes for movement of the Cp rings among the different C_{2h} structures shown in Table II are not huge, but on the order of 10–20 kcal/mol. As we shall see later, such steric repulsions are large enough to affect the geometry of the complex along a coordinate where bond strength contributions may be this same order of magnitude, such as the metal–metal coordinate. However, they cannot be the overriding factor in comparing the short Zr–Zr distance in **4**, compared to **1** and **2**, where the deciding factor must be the strength of the metal-bridging ligand bond. We explore the relative strengths of the metal–metal and metal–ligand bonds near the end of this manuscript when we take up fragmentation energies.

In order to further explore the utility of the molecular mechanics model for these complexes, we have gone beyond the above studies which examined the relative energies of fixed-geometry Cp rings. In brief we found that this model is not useful to understanding the geometry of the Zr_2X_2 framework but that it is helpful to rationalize the geometry of the Cp rings on the Zr atoms and with each other. We now describe some of the computational exercises that we did to come to this conclusion.

We first used the "generalized" force field in PCMODEL to examine also the geometrical features of the Zr_2X_2 framework as it is attached to the Cp rings. We employed a "generalized" metal atom with an atomic radius of 1.60 Å. The force field for the P atom in PCMODEL 4.0 is not complete, so no optimizations involving that portion of **1** could be done. Instead we completed optimizations of the Zr(IV) compounds **3** and **4** and of Zr(III) compounds related to **1**, but with the X group being SH and Cl instead of PH_2. We found that for a given structure, if we indicate in building the force field that there is a Zr–Zr bond, this distance optimizes to about 3.2 Å. If we indicate that there is no Zr–Zr bond, the Zr–Zr distance optimizes to something near 3.8 Å; whether the complex is formally Zr(III) or Zr(IV) is unimportant.

In a second set of exercises we constrained the Zr_2X_2 framework to its experimental structure for **1** and **4** and then optimized the CNT–Zr–CNT angle; the optimized angle we obtained was 130° for **1** and 125° for **4**. These are very near the actual structures found in the complexes (Table I). (In the experimental structures there are R groups on the P and N bridging ligands, rather than the H atoms that we have in our model compounds.)

In a third set of molecular mechanics exercises, we replaced the H atoms in the model μ-PH_2 ligand with CH_3 groups, as found in the actual complex **1**. We employed a P–C distance of 1.90 Å and a C–P–C angle of 93°. We initially used experimental metrical parameters for the remainder of structure **1** and then performed rotation around the P–C bond so as to allow the H atoms of CH_3

(36) H···H nonbonded distances of 1.83 and 2.04 Å have been reported in a sterically congested compound containing Cp*CpZr: Elsner, F. H.; Tilley, T. D.; Rheingold, A. L.; Geib, S. J. *J. Organomet. Chem.* **1988**, *358*, 169. See also Brock, C. P.; Minton, R. P. *J. Am. Chem. Soc.* **1989**, *111*, 4586.

to find their optimal location with respect to near-neighbor H atoms on the Cp rings, in C_{2h} geometry of the Cp rings. We found surprisingly close contacts between these H atoms: an H atom on each CH_3 has one near-neighbor contact with an H on Cp of 2.0 Å and another of 2.1 Å. We then "froze" the Zr_2X_2 portion of the molecule and optimized the Zr–CNT distance and the CNT–Zr–CNT angle. Compared to these optimized values for R ≡ H (2.15 Å and 130°, respectively), we found that Zr–CNT had increased to 2.18 Å and that CNT–Zr–CNT had decreased to 125°. These two changes have the effect of increasing the above mentioned near-neighbor H···H contacts to 2.1 and 2.2 Å. The shifts in Cp positions, due to the addition of CH_3 instead of H on the bridging phosphido ligand, shows that these methyl groups have a steric effect on the overall geometry of 1. The near-neighbor H···H contacts quoted above are very close to those reported in Table II, for distances between H atoms on different Cp rings. Hence, part of the explanation for the long Zr–Zr distance could be due to these contacts of the Cp rings with the methyl groups of the bridging phosphido ligand.

Frontier Orbitals of the Fragment Moieties of 1, 2, and 4. In Figure 1 we present the frontier molecular orbitals of Cp_2Zr and $(Cp_2Zr\text{–}ZrCp_2)^{2+}$. We first look at the left side of Figure 1 to see the frontier orbitals of the Cp_2Zr fragment (C_s symmetry, C_{2v} results are nearly identical). Our results, both for the relative orbital energies and for the orbital character, are similar to the extended Hückel results on the model fragment Cp_2Ti.[37] Important orbitals for our discussion are the two orbitals labeled 1a′ and 2a′. We will refer to the former as a "sideways" z^2 orbital; the latter is best described as a diffuse "dsp" hybrid. These two orbitals are within 0.1 eV in neutral $ZrCp_2$, if 1a′ is given an occupation of two electrons and 2a′ is given none. (In $ZrCp_2^+$ these orbitals differ in energy by about 1 eV.)

We now turn to the frontier orbitals that arise when the two $ZrCp_2$ units are brought together. Consider $ZrCp_2^+$ (d^1) so that the electron count is correct to form a Zr–Zr bond (distance at 3.65 Å), as in the final μ-PR_2 or μ-I compound. The second panel of Figure 1 shows the frontier orbitals that result from bringing together the two C_s fragments so as to form a C_{2h} fragment with staggered Cp rings. The HOMO (an a_g orbital in C_{2h} symmetry) of $(Cp_2Zr\text{–}ZrCp_2)^{2+}$ consists of 65% 1a′ orbitals and 35% 2a′ orbitals of the $ZrCp_2$ fragments. We display a contour diagram of this orbital in Figure 2. It is clear that this orbital comprises the expected Zr–Zr bond. Since the 2a′ orbitals (dsp hybrids) on each fragment are so diffuse, they overlap strongly with each other and hence predominate over the 1a′ fragment orbitals so that this orbital looks like a strongly directed σ bond.

Frontier Orbitals of 1. In Figure 3 we depict the eigenvalues for 1, which result from bringing together the frontier orbitals of the fragments $(Cp_2Zr\text{–}ZrCp_2)^{2+}$ and $[(PH_2)_2]^{2-}$. There is a sizable gap (~2 eV) between the HOMO Zr–Zr σ bonding orbital ($2a_g$) and the Zr–Zr σ^* antibonding orbital ($2b_u$). This by itself is indicative (but not proof) of a closed-shell ground state and the formation of a Zr–Zr bond. In Figure 4 we exhibit pertinent information for these orbitals as well as the other four occupied orbitals ($1a_g$, $1a_u$, $1b_u$, $1b_g$) shown in Figure 3. The numbers and pictures shown in Figure 4 are self-explanatory and so we do not dwell on them. Instead we turn our attention to the nature of the HOMO.

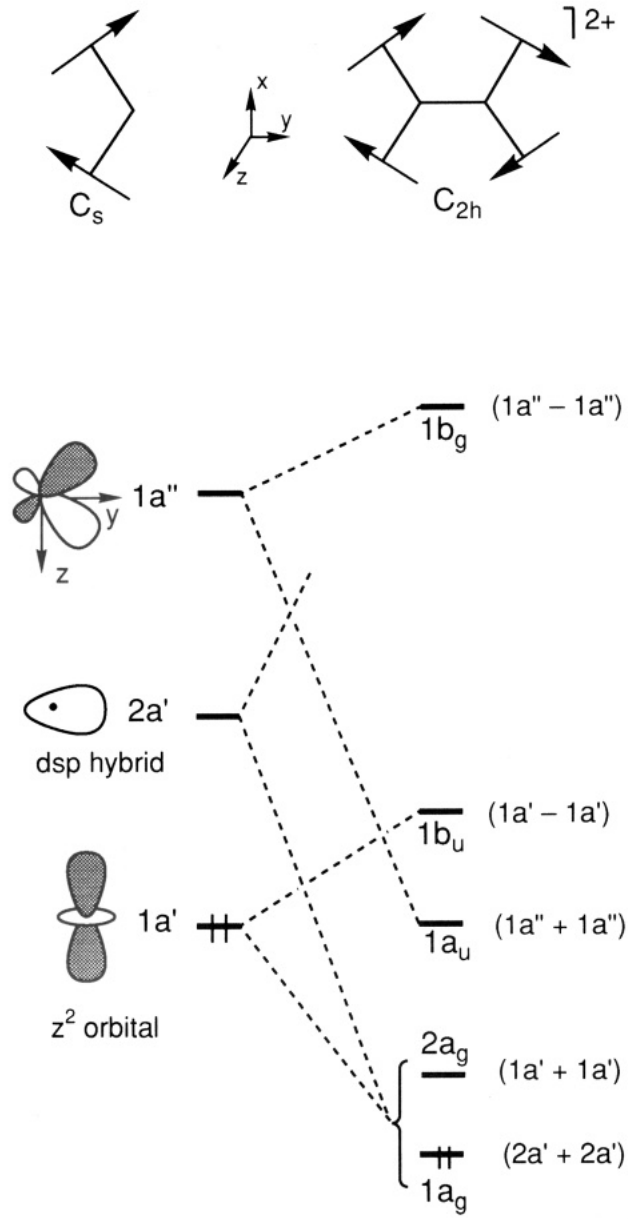

Figure 1. Qualitative molecular orbital sketch for MCp_2 and $(Cp_2MMCp_2)^{2+}$. The three frontier orbitals of $ZrCp_2$ are nearly degenerate, lying between −1.85 and −1.65 eV. For the dication, the levels are also close in energy, with splittings of about 0.1 eV, except for $1b_g$, which is split from $1b_u$ by about 1 eV. The orbitals for the dication range between −9.3 eV for the uppermost orbital down to −10.50 eV for the $1a_g$ orbital. As discussed in the text, the $1a_g$ and $2a_g$ orbitals contain significant components of both 1a′ and 2a′. For the neutral dimer, both $1a_g$ and $2a_g$ occupied, this is not the case and we find that $1a_g$ is nearly 90% 2a′ and $2a_g$ is nearly 90% 1a′, hence the notation that we have made to the right of these orbitals.

We exhibit the orbital diagram for the HOMO ($2a_g$, Zr–Zr bond) of the μ-PH_2 compound (1) in Figure 5. This orbital has all the marks of a metal–metal bond, but it is important to note that it has a decidedly altered character from that shown in Figure 2 for the prototype d^1–d^1 bond of the model fragment $(Cp_2ZrZrCp_2)^{2+}$. Although there is a metal–metal interaction, it is formed from two "sideways" z^2 orbitals and not from the diffuse dsp hybrids pointing at each other; the $ZrCp_2^+$ contribution to this $2a_g$

(37) Lauher, J. W.; Hoffmann, R. *J. Am. Chem. Soc.* **1976**, *98*, 1729.

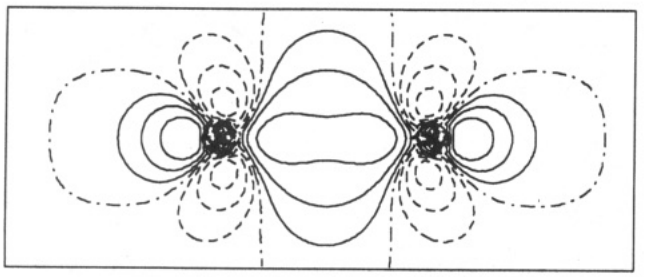

Figure 2. Constant contour values for the highest occupied molecular orbital of $(Cp_2Zr)_2^{2+}$, in the *yz* plane. The solid lines represent positive amplitude, and the dashed lines, negative amplitude. The dash–dot line is the nodal line. The values of the contours are 0.05, 0.1, and 0.2 electrons/(bohr)^3.

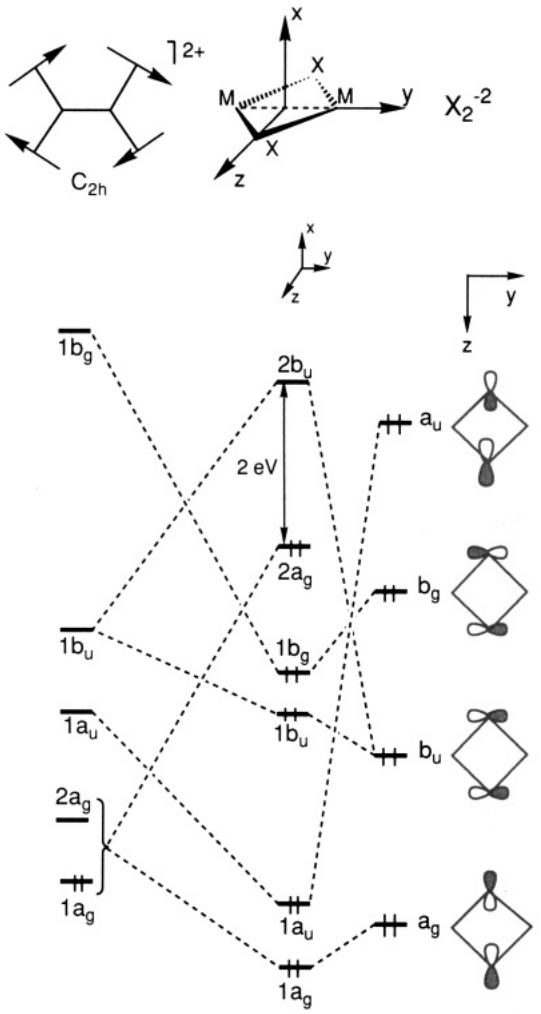

Figure 3. Qualitative molecular orbital sketch for $(Cp_2Zr)_2^{2+}$, $[Cp_2Zr(\mu\text{-}PH_2)]_2$, and X_2^{2-}. The M_2X_2 atoms lie in the *yz* plane. The energy scales in each of the three columns are shifted relative to each other due to the large Coulomb effect of comparing neutrals, cations, and anions. Hence, this diagram is mainly of use in checking the symmetry of the frontier orbitals.

orbital is 86% 1a′ and only 1% 2a′. (See the left panel of Figure 1 for a sketch of these fragments orbitals.) This is in sharp contrast to the case of the model fragment $(Cp_2ZrZrCp_2)^{2+}$ where we recall that the HOMO was 65% 1a′ and 35% 2a′. The 2a′ contribution is now distributed between $1a_g$ (Zr–Zr bonding) and $1b_u$ (Zr–Zr antibonding); its net contribution to metal–metal bonding has been squelched by the presence of the bridging ligands, although it does contribute to the metal–ligand bonding.

The result is that the HOMO of 1 is not expected to provide a strong metal–metal bond. We discuss the energetic contribution of this orbital in the section on fragmentation energies below. For the moment we make some qualitative remarks about this orbital. The overlap integral of the 1a′ orbital on each $ZrCp_2^+$ fragment ("sideways" z^2, see the $2a_g$ orbital sketch of Figure 4) amounts to only 0.07. This is only $\sim 1/2$ as large as that of two z^2 orbitals facing each other "end-on", and hence we might expect the d orbitals to be able to contribute only $\sim 1/2$ of their possible potential to the Zr–Zr bond.[38] This underscores the weakness of the interaction between the two "sideways" z^2 orbitals.

The reason why the 2a′ orbital of $ZrCp_2$ (diffuse "dsp hybrid") is not involved in the HOMO of 1 is readily apparent when one examines the overlap of the 1a′ and 2a′ fragment orbitals with the a_g fragment orbital of the bridging ligand. These overlap integrals are shown next to the sketches of the $1a_g$ and $2a_g$ orbitals in Figure 4. The 1a′ orbital of $ZrCp_2$ overlaps with the a_g PH_2 combination with a value of 0.06, whereas 2a′ has a much larger value of 0.33. The result is that 2a′ becomes involved in the low-lying $1a_g$ orbital of 1, whereas 1a′ does not contribute to this orbital. Hence 1a′ is available for the compound $2a_g$ orbital (HOMO), whereas the component of 2a′ not utilized in the $1a_g$ orbital is pushed into antibonding orbitals.

In order to investigate further the nature of the bonding of 1 we have computed two density difference maps, as shown in Figure 6a,b. In the first we take the total electron density of 1 and subtract from it the fragment densities of two $ZrCp_2^+$ [$(1a')^1$ occupation] and of two PH_2^- fragments. This density difference map (Figure 6a) looks very similar to that published by Rohmer and Bénard.[27] It shows a large *buildup* of electron density that is "X" shaped in the Zr_2P_2 plane. We do not feel that this map by itself provides evidence for a Zr–Zr bond in 1, since it can just as well be interpreted as a P–P bond.

In order to obtain a different viewpoint, we provide another density difference map in Figure 6b. In this diagram we take the total electron density of 1 and subtract from it the fragment densities of $(Cp_2ZrZrCp_2)^{2+}$ and of two PH_2^- fragments. This map looks decidedly different from the first one. Now we see a *depletion* of electron density out of the Zr–Zr region and into the Zr–P region. The differences between the description provided by Figure 6a,b are understandable on the basis of the nature of the difference between the HOMO of $(Cp_2ZrZrCp_2)^{2+}$ and of 1, a point which we emphasized above. It is noteworthy that the density difference map of neither Figure 6a nor Figure 6b clearly shows a Zr–Zr bond, as shown from the HOMO of $(Cp_2ZrZrCp_2)^{2+}$ in Figure 2. We take Figure 6a,b as evidence for the lack of involvment of the 2a′ fragment orbitals of $ZrCp_2$ in the Zr–Zr bonding of 1. In summary, these density difference maps alone do not tell us much about the nature of the Zr–Zr bonding,

(38) We computed the value of the overlap for end-on and sideways in order to verify this comment about the overlap being only $\sim 1/2$ as large. A justification for the remark about the qualitative relationship between overlap and bond energy comes from perturbation theory for degenerate orbitals, see for example: Burdett, J. K. *Molecular Shapes*; Wiley-Interscience: New York, 1980. If one applies the extended Hückel expression with $K = 2.0$ for the off-diagonal term that couples the two degenerate orbitals, one readily finds that the bonding orbital expression is $e_1 = e_1^0[(1 + 2S_{12})/(1 + S_{12})]$. For small values of S_{12} ($\sim$0.1), one can readily see that e_1 is approximately $e_1^0(1 + S_{12})$. Since there are two electrons in this bonding orbital, the electronic energy is stabilized by $2S_{12}$.

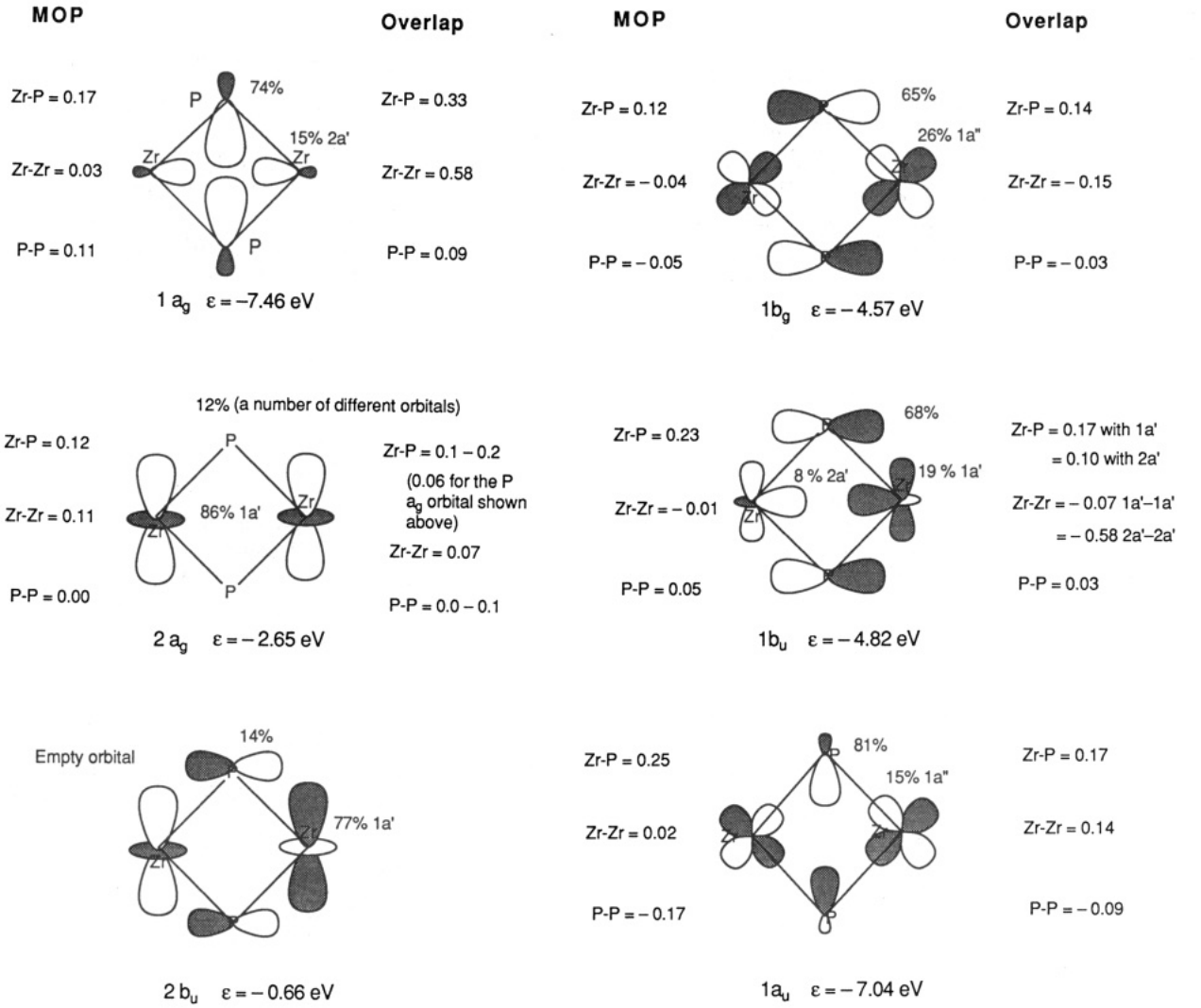

Figure 4. Qualitative sketches of the frontier orbitals of $[Cp_2Zr(\mu\text{-}PH_2)]_2$. The heading MOP refers to the Mulliken overlap population, and "overlap" refers to the value of the overlap integral between the fragment orbitals of $ZrCp_2$ and PH_2 as indicated. The eigenvalues of these orbitals are also displayed.

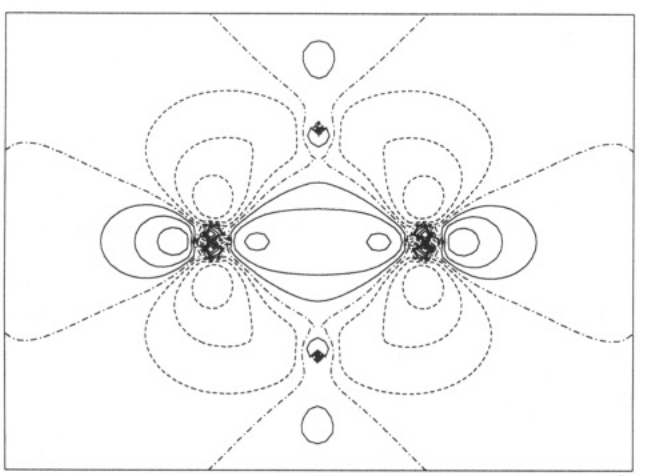

Figure 5. Constant contour values for the highest occupied molecular orbital of $[Cp_2Zr(\mu\text{-}PH_2)]_2$, in the *yz* plane. The position of the Zr atoms is clearly ascertained along the horizontal axis and the P atoms are along the vertical axis. Other comments apply as per Figure 2.

mainly because of the entanglement of the bridging atoms. We will further examine the nature of the Zr–Zr interaction below, after we have examined the HOMO for the μ-I compound.

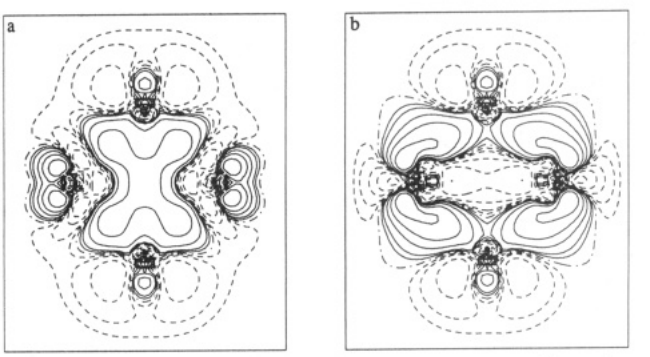

Figure 6. (a) Electron density difference map (*yz* plane) for $[Cp_2Zr(\mu\text{-}PH_2)]_2$ minus the electron density of two $ZrCp_2^+$ and two PH_2^- fragments. The position of the Zr atoms is clearly ascertained along the horizontal axis and the P atoms are along the vertical axis. Solid lines indicate a positive value of electron density and dashed lines indicate a negative value. The dash–dot line is the nodal line. The values of the contours are 0.001, 0.002, 0.005, 0.01, 0.02, 0.05, and 0.1 electrons/(bohr)^3. (b) Same as (a) except the density difference is with respect to the fragments $(Cp_2Zr)_2^{2+}$ and two PH_2^- groups. Other comments apply as for (a).

Bonding in 2. The bonding picture for the μ-I compound (**2**) is sufficiently different from that of μ-PH_2 (**1**) so that we discuss it briefly. The HOMO is presented

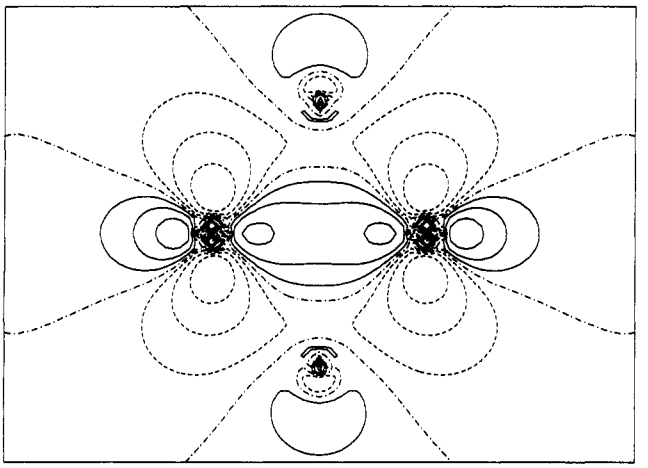

Figure 7. Constant contour values for the highest occupied molecular orbital of $[Cp_2Zr(\mu\text{-}I)]_2$, in the *yz* plane. The position of the Zr atoms is clearly ascertained along the horizontal axis, and the I atoms are along the vertical axis. Other comments apply as per Figure 2.

Table III. Mulliken Population Analysis and Dissociation Energies, *D* (kcal/mol), to Fragments[a]

compd	q(M)	$q(\mu\text{-}X_f)$	MOP-(M_f–X_f)	MOP-(M_f–M_f)	*D*
1^{2+} [b] (with no μ-X^-)	1.15	(−1)		0.38	
1 (μ-PH_2)	1.20	−0.19	1.42	−0.05	251
1^{2+} (μ-PH_2)	1.07	0.02	1.35	−0.22	
1^{2-} (μ-PH_2)	1.32	−0.47	1.72	0.02	
2 (μ-I)	0.79	0.04	0.90	0.05	273
2^{2+} (μ-I)	0.60	0.30	1.34	−0.18	
2^{2-} (μ-I)	1.04	−0.22	−0.32	0.04	
4 (μ-NH)	1.69	−0.67	1.20	−0.46	376
4^{2-} (μ-NH)	1.68	−0.68	0.97	−0.38	
6 (M = Ti, μ-Cl)	0.88	−0.20	0.96	−0.05	294

[a] MOP ≡ Mulliken overlap population; X_f refers to the entire bridging ligand M_f refers to MCp_2. [b] This first line is for $Cp_2ZrZrCp_2^{2+}$.

in Figure 7. Since the Zr–I distance is somewhat longer than the Zr–P distance, what was one nodal line between the P nucleus and the midpoint of the Zr–Zr bond (Figure 5) has now turned into *two* nodal lines. The wide distance between these lines would seem to indicate that this orbital is antibonding between $ZrCp_2$ and I, a feature which is confirmed by a Mulliken population analysis of this orbital.

Mulliken Population Analysis of 1 and 2. The Mulliken population analysis data are presented in Table III. For **1** and **2** we find a large positive Mulliken overlap population between the bridging ligands and the metal fragments, 1.42 and 0.90, respectively. However, the value for the metal–metal fragments is at first surprising; for **1** we find a slightly negative Cp_2Zr–$ZrCp_2$ overlap population and for **2** it is just slightly positive, −0.05 and +0.05, respectively. This is in contrast to the large positive overlap population (0.38) between the $ZrCp_2^+$ fragments for the model system $(Cp_2Zr\text{–}ZrCp_2)^{2+}$ (first line of Table III). These differences between metal–metal overlap populations fit with what we have said above about the contrasting nature of the bonding in **1** and **2** compared to $(Cp_2Zr\text{–}ZrCp_2)^{2+}$. We now amplify that statement in the next paragraph.

Why is the metal–metal fragment Mulliken overlap population of **1** and **2** so miniscule in the face of the evidence regarding orbital contour diagrams of the HOMO (Figures 5 and 7)? First, the HOMO is only one of five orbitals that mainly are involved in the bonding of the M_2X_2 moieties (Figures 3 and 4). A positive Zr–Zr Mulliken overlap population in one orbital is canceled by corresponding antibonding components from one or more of the underlying (four) occupied orbitals that are involved in holding these fragments together. This effect is clearly seen from the data given in Figure 4. Notice in particular how the $1b_u$ orbital cancels the $1a_g$ orbital as regards Zr–Zr bonding. Second, as seen in the density difference map of Rohmer and Bénard,[27] and in our own (Figure 6a), there is an accumulation of electron density at the midpoint of the Zr–Zr axis, compared to the fragments of $ZrCp_2^+$ and PH_2^-. But at the same time there are *depletions* of electron density between this midpoint and each Zr atom. Third, the density difference map shown in Figure 6b shows that electron density along the Zr–Zr axis in $(Cp_2Zr\text{–}ZrCp_2)^{2+}$ is moved into the Zr–P region of **1**. The shift of electron density out of the Zr–Zr region and into the Zr–X region lowers the Zr–Zr Mulliken overlap population until it is near zero.

Bonding in 4. We now describe the bonding in the μ-NH compound, **4**. This compound is formally Zr(IV), and hence there are insufficient electrons to form a Zr–Zr bond. The bonding pattern is not unlike that shown in Figure 3 for the μ-PH_2 compound, except that the $2a_g$ orbital is now empty. Even so, the lack of two electrons does not imply that **4** cannot obey the 18-electron rule, since the μ-NH ligand of **4** is more likely to donate π electrons to the metal than is the μ-I ligand of **2**. This can be seen by looking at the formal charges of the atoms in the M_2X_2 plane, **9**. (Note that in Figure 1 we treated the

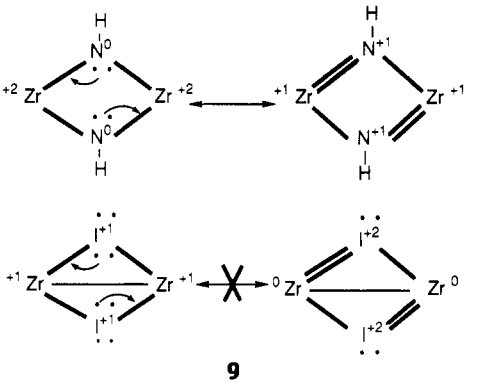

9

bridging groups X as anions in building up the complex. However, in **9** we present the bridging groups as covalently bonded to the metal atoms in the M_2X_2 framework. In both Figure 1 and in **9** we treat the Cp ligands as formal anions.)

We take the μ-I atom as our example; its formal charge is +1, as shown in **9**, and so it is unlikely to donate π electrons to the Zr^+ center. However, the μ-NH ligand of **4** has a formal charge of zero and it likely will donate π electrons to Zr^{2+}. In fact, our Mulliken population analysis shows that this is exactly what has happened. The iodine π orbitals (i.e., perpendicular to the Zr_2X_2 plane) in the iodo compound have an occupation of 1.90 whereas those of the NH compound are only 1.55 electrons.

As stated earlier, the main difference between the electronic structure of **1** and **2** compared to **4** is that the $2a_g$ orbital is empty. This has several important consequences. (1) π donation from the bridging ligands becomes possible because the formal charge on the metal is high, as just discussed. (2) The metal atoms have a low-lying empty orbital ($2a_g$) that allows for a donor ligand to participate in the bonding to the Zr atom. In fact, such

a compound has been prepared[39] with a μ-NNR_2 ligand; this compound otherwise is like the model μ-NH compound shown in **4**. The β nitrogen atom "wraps around" and its lone pair orbital donates electron density to an adjacent Zr atom. (3) Besides the ability of a ligand donor atom to attach itself to the Zr atom, it might be possible to reduce the complex and form the dianion, as this process could form a Zr–Zr bond. We now examine results for such a proposed dianion of **4** along with results for the dications and dianions of **1** and **2**.

Dications and Dianions of 1, 2, and 4. We have completed theoretical studies of several dications and dianions in order to help us better understand the nature of the frontier orbitals of these complexes. We begin with the data for **4** and $\mathbf{4}^{2-}$, as found in Table III. The metal–metal Mulliken overlap population is increased slightly in $\mathbf{4}^{2-}$ compared to **4**. The fact that the Mulliken overlap population of the Zr–Zr bond did not increase much when two electrons were added to $2a_g$ is a further indication of the weakness of this orbital vis-a-vis Zr–Zr bonding. This $2a_g$ orbital, for **1**, **2**, and $\mathbf{4}^{2-}$, can best be viewed as a place for the molecule to "park" two electrons. The interaction is strong enough to cause pairing of electrons, but because of the "sideways" orientation of the fragment orbitals, there is not a large increase of electron density in the Zr–Zr region.

Table III also presents data for $\mathbf{1}^{2+}$ and $\mathbf{1}^{2-}$. Removal of two electrons from the $2a_g$ orbital of **1** to form $\mathbf{1}^{2+}$ causes the metal–metal fragment overlap population to decrease whereas the overlap population to the bridging fragments is hardly affected, both as expected on the basis of the sideways z^2 character of the HOMO shown in Figures 4 and 5 for **1**. Addition of two electrons to the LUMO of **1** to form $\mathbf{1}^{2-}$ *increases* both types of overlap populations. For a sketch of this orbital see **10**.[40] Its eigenvalue lies

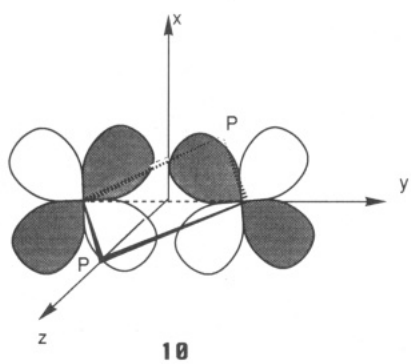

10

about midway between $1b_u$ and $2b_u$, and it consists of a Zr–Zr π orbital perpendicular to the Zr_2P_2 plane. It is of $xy + xy$ character. In summary, the data in Table III indicate that **1** should survive electrochemical oxidation or reduction since the metal-bridging ligand overlap populations are not drastically affected.

We now discuss the results in Table III for $\mathbf{2}^{2+}$ and $\mathbf{2}^{2-}$. The oxidation of **2** to form its dication substantially *increases* the Zr–I overlap population; this increase fits with the comments made about the antibonding Zr–I character of the HOMO for **2**; see Figure 7. The situation is the opposite for the reduction of **2** to form $\mathbf{2}^{2-}$; the data in Table III show there is a dramatic decrease in the Zr–I Mulliken overlap population, so that we expect reduction by two electrons to destroy the compound. The HOMO of $\mathbf{2}^{2-}$ (LUMO of **2**) is the $2b_u$ molecular orbital. A mental picture of this orbital can be garnered by looking at the sketch of $2b_u$ of **1**, shown in Figure 4. This orbital is indeed strongly Zr–X antibonding. (We insert a note of caution about the prediction that the reduction of **2** will destroy the complex. This is because the $2b_u$ orbital and the Zr–Zr $(xy + xy)$ π orbital (**10**) of $\mathbf{2}^{2-}$ are nearly degenerate. That is, if these two orbitals were to change energetic order, the electronic structure of $\mathbf{1}^{2-}$ is predicted to be the same as that of $\mathbf{2}^{2-}$.)

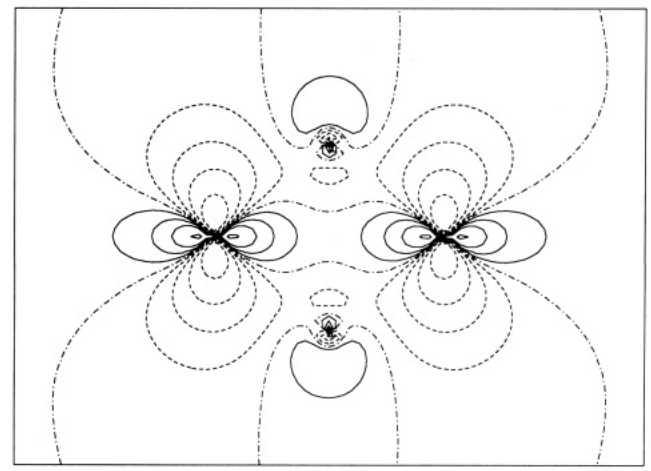

Figure 8. Constant contour values for the highest occupied molecular orbital of $[Cp_2Ti(\mu\text{-}Cl)]_2$, in the yz plane. The position of the Ti atoms is clearly ascertained along the horizontal axis, and the Cl atoms are along the vertical axis. Other comments apply as per Figure 2.

The data in Table III reveal one other interesting piece of information about **1**, **2**, and **4** along with the various dications and dianions that we have discussed. The Mulliken charge on the metal atom and on the bridging ligand sums to nearly "one" in all cases. That is, the Cp rings are functioning as effective electron "buffers" in these systems.

Bonding in the Titanium Complex, 6. Recall from the Introduction that this compound exhibits antiferromagnetic behavior and that it has a long Ti–Ti bond distance of about 3.96 Å. Data for this compound are included in Table III. The electronic structure of the frontier orbitals is markedly different from those for **1** and **2**. In the latter two cases the σ–σ^* gap was $\sim$2 eV. For **6** it is only about 0.2 eV when the calculation is carried out closed shell.

In Figure 8 we display the orbital contour of the HOMO $2a_g$ orbital with an occupation of two electrons in this orbital. There is a dramatic contrast between this orbital and that shown in Figures 5 and 7 for **1** and **2**, respectively. It is clear that the 3d orbital of Ti is very contracted compared to the 4d of Zr. As a result there is very meager overlap between the two "sideways" z^2 orbitals. It is not at all surprising that the molecule exhibits magnetic activity.[22] We have probed this point further by calculation of the Heisenberg constant J as outlined by Noodleman and Baerends.[41] We find the ferromagnetically and antiferromagnetically coupled states [i.e., the triplet and singlet states of the configuration $(2a_g)^1(2b_u)^1$]

(39) Walsh, P. J.; Carney, M. J.; Bergman, R. G. *J. Am. Chem. Soc.* **1991**, *113*, 6343.

(40) Cotton and co-workers[6b] report the same kind of LUMO in their complex that we find for **1**.

(41) Noodleman, L.; Baerends, E. J. *J. Am. Chem. Soc.* **1984**, *106*, 2316.

Table IV. Fragmentation Energies for $(Cp_2Zr-ZrCp_2)^{2+}$ and $(Cp_2Zr-ZrCp_2)^0$ (kcal/mol)

computation[a]	$(Cp_2Zr-ZrCp_2)^{2+}$	$(Cp_2Zr-ZrCp_2)^0$
complete basis	−54	+49
all virtual a′ eliminated, except 2a′	−60	+38
all virtual a′ kept, except 2a′	−83	+5
all virtual a′ eliminated		−3

[a] The a′ orbitals here refer to those on the $ZrCp_2$ fragment.

to be degenerate to within the accuracy of the calculation. According to the experimental Heisenberg J value of −111 cm^{-1}, the singlet should be slightly favored.

Fragmentation Energies. Table III presents calculated fragmentation energies of $[Cp_2M(\mu\text{-}X)]_2$ to two Cp_2M and two X. The fragmentation energies are large and range from 251 to 376 kcal/mol. In line with our discussion of the Mulliken overlap populations presented in Table III, we might expect that most of this dissociation energy is due to the metal–ligand bonding and that very little is due to metal–metal bonding. In this section we present the results of some theoretical studies that we have completed in an attempt to unravel the contribution of the $ZrCp_2$ fragment orbitals 1a′ and 2a′ to the overall fragmentation energies.

We begin with a series of theoretical studies on $(Cp_2Zr-ZrCp_2)^{2+}$ and on $(Cp_2Zr-ZrCp_2)^0$. Three results for the fragmentation energies of the dication are presented in Table IV. In this moiety there is a formal single Zr–Zr bond; the $1a_g$ orbital is occupied (Figure 1). We first completed a study of the dication by making use of the complete set of basis orbitals on each $ZrCp_2^+$ fragment. This results in a computed fragmentation energy to two $ZrCp_2^+$ fragments of −54 kcal/mol. That is, the two fragments are unbound. This is not surprising in view of the positive charge on each fragment. (The situation can be considered akin to that in He_2^{2+}, which has been shown to have a bond but to be metastable with respect to two He^+.[42]) If we eliminate all of the virtual a′ orbitals except for the empty 2a′ orbital (diffuse dsp hybrid) from the basis set of $ZrCp_2^+$, we find that the dication is destabilized by (only) an additional 6 kcal/mol. If we eliminate only the 2a′ orbital and keep all the higher a′ virtual orbitals, the dication is destabilized by 29 kcal/mol relative to the full basis calculation. These results indicate that of all the virtual a′ orbitals on $ZrCp_2^+$, the diffuse dsp hybrid (2a′) is most important for the (metastable) bond in the dication complex. To further examine the contribution of 2a′ to the metal–metal bond, we also have completed theoretical studies on the neutral $(Cp_2Zr-ZrCp_2)^0$.

Table IV lists a series of four calculations that we did to determine the fragmentation energy of the neutral dimer to two neutral $ZrCp_2$ fragments. The $1a_g$ and $2a_g$ frontier orbitals are now occupied (Figure 1). The first three calculations on the neutral dimer correspond exactly to the three just mentioned for the dication. We find that with all basis orbitals included, the fragmentation energy is +49 kcal/mol. Hence we can state that a combination of 1a′ + 1a′ and 2a′ + 2a′ produces a total bond energy of 49 kcal/mol. (For purposes of future discussion we will call this 50 kcal/mol.) Eliminating all virtual a′ orbitals except 2a′ decreases this to 38 kcal/mol. Eliminating 2a′ but keeping all other virtual a′ orbitals drops the bond energy dramatically to 5 kcal/mol. Finally, eliminating *all* virtual a′ orbitals produces an unstable dimer with a bond energy of −3 kcal/mol. These results again indicate that all virtual a′ orbitals except 2a′ are not too important.

From the results of the previous two paragraphs we cannot say how much of the 50 kcal/mol bond energy is due to 1a′ and how much is due to 2a′. This is because when we remove the 2a′ orbital from the basis, the antibonding combination of the 1a′ orbitals is occupied of necessity, and hence this eliminates their contribution to the bonding as well. We could partition the 50 kcal/mol bond energy equally between contributions due to 1a′ and due to 2a′ and say that each is worth roughly 25 kcal/mol. Another approach would be to say that, since the overlap integral of (1a′, 1a′) is only 0.07 and that of (2a′, 2a′) is 0.58, the bond energy contribution should be partitioned in direct proportion to the overlap integral, as we discussed in footnote 38. In this approach we might then suggest that the 1a′ orbital contributes only about 5 kcal/mol and that the 2a′ contributes about 45 kcal/mol.

Table III shows that the fragmentation energy of 1 to two $ZrCp_2$ and two PH_2 is 251 kcal/mol. We did one additional theoretical study on compound 1 besides this full basis study that has been examined throughout this manuscript. In that additional study we eliminated all virtual a′ orbitals from the basis of the $ZrCp_2$ fragment. Doing so resulted in a drop in the fragmentation energy from 251 to 224 kcal/mol. This is only about half as much as the drop in fragmentation energy when all the virtual a′ orbitals were eliminated in the neutral fragment $(Cp_2Zr-ZrCp_2)^0$. So we can say that the virtual 2a′ orbital, which contributes most of the virtual a′ contribution, provides about 10% (25 kcal/mol) of the bond energy in 1. How much of this is due to Zr–Zr bonding and how much to Zr–X bridge bonding is a point that we cannot answer.

We agree partially with Mason and Mingos[43] that it is impossible to unravel the metal–metal bonding from the metal–ligand bonding in these metal–bridge situations. The results that were discussed in the previous paragraph show that the fragmentation energy of 1 (251 kcal/mol) is due mainly to metal–ligand bonding and that very little is due to the metal–metal bonding. We can make this statement on the basis of our studies reported in Table IV, which show that the contribution of interaction of two sideways z^2 orbitals to the bonding is worth at most 25 kcal/mol. (This comment uses the assumption that the 50 kcal/mol bond dissociation energy of $(Cp_2Zr-ZrCp_2)^0$ can be equally partitioned between 1a′ and 2a′, a very generous statement given the small overlap of the 1a′ orbitals with each other.)

The comment that the metal–metal bond contributes about 25 kcal/mol to the fragmentation energy also makes it clear why the metal–metal distance is such a flexible part of the structure of these molecules. Recall that we estimated the van der Waals' repulsions among the four Cp groups to be on the order of 10–20 kcal/mol for these molecules. This means that both the vdw repulsions and the metal–metal bond contribute about the same amount but with opposite sign to the stability of these complexes. But, in the big picture of the total fragmentation energies reported in Table III, these are very small numbers. That is, the metal–ligand bond strength is the overriding term that determines the total fragmentation energies.

(42) Guilhaus, M.; Brenton, A. G.; Beynon, J. H.; Rabrenovic, M.; von R. Schleyer, P. *J. Chem. Soc., Chem. Commun.* **1985**, 210.

(43) Mason, R.; Mingos, D. M. P. *J. Organomet. Chem.* **1973**, *50*, 53.

Summary Regarding the Nature of the Metal–Metal Bond. (1) The interaction of the frontier orbitals of $ZrCp_2$ in **1** and **2** is sufficiently strong to provide a large HOMO–LUMO gap. (2) The HOMO of **1** and **2** consists of "sideways" bonding z^2 orbitals that have a weak overlap, but strong enough to cause spin pairing of the two electrons. (3) The bridging ligands cause a depletion of electron density along the Zr–Zr direction, so that whatever Zr–Zr bonding is present is much less than it would have been in the absence of the bridging ligands (Figure 6b). (4) To further examine the nature of the Zr–Zr bond, we have completed a Mayer bond order analysis[44] within the Fenske–Hall method[45] for compound **1**. We find a Zr–Zr bond order of 0.55, in agreement with the other comments we have been making about this bond. It is a bond in the sense that the electrons are spin paired. But it is a rather feeble bond in the sense that the atomic orbitals are not strongly overlapping. Hence we feel comfortable with a bond order of about 0.5. (5) Bond distance is not a good criterion of bond order for these bridging ligand systems, because it does not take into account the atomic size of the bridging ligands or the steric requirements of the Cp rings in such complexes. (6) It is impossible to unravel completely the metal–metal bonding from the metal–ligand bonding in these bridging complexes. But by judicious calculations with and without bridging ligands, and with and without pertinent basis orbitals on the fragments, we have been able to show that the metal–metal bond contributes very little to the overall fragmentation energy of these complexes. This statement is in agreement with the shallow potential energy curves for the metal–metal coordinate that Rohmer and Bénard have found in their computational studies.[28]

(44) Mayer, I. *Chem. Phys. Lett.* **1988**, *148*, 95 and references therein.
(45) Fenske, R. F. *Pure Appl. Chem.* **1971**, *27*, 61. Hall, M. B.; Fenske, R. F. *Inorg. Chem.* **1972**, *11*, 768.

Acknowledgment. The authors wish to thank Marc Bénard for sending preprints of the manuscripts in refs 27 and 28. Thanks are also due to NATO for a Collaborative Research Grant (No. 870025) and to the National Science Foundation for a grant to Calvin College (CHE-8822535). R.D.K. thanks Calvin College for a Calvin Research Fellowship which provided for released time to work on this project.

OM920314Y